

UC Davis

UC Davis Previously Published Works

Title

Integrated analysis of flow, form, and function for river management and design testing

Permalink

<https://escholarship.org/uc/item/6gs628cs>

Journal

Ecohydrology, 11(5)

ISSN

1936-0584

Authors

Lane, Belize A
Pasternack, Gregory B
Solis, Samuel Sandoval

Publication Date

2018-07-01

DOI

10.1002/eco.1969

Peer reviewed

1 **Integrated analysis of flow, form, and function for river**
2 **management and design testing**

3

4 **Belize A Lane^{1*}, Gregory B Pasternack² and Samuel Sandoval-Solis²**

5

6 *Corresponding author

7 Email: belize.lane@usu.edu

8 ¹ Department of Civil and Environmental Engineering, Utah State University, Logan, Utah USA

9 ² Department of Land, Air and Water Resources, University of California Davis, California USA

10

11

12 Cite as:

13 Lane, B.A., Pasternack, G.B., and Sandoval-Solis, S. 2018. Integrated analysis of flow, form, and
14 function for river management and design testing. *Ecohydrology*. DOI:10.1002/eco.1969

15

16 Abstract

17 The extent and timing of many river ecosystem functions is controlled by the interplay of
18 streamflow dynamics with the river corridor shape and structure. However, most river
19 management studies evaluate the role of either flow or form without regard to their dynamic
20 interactions. This study develops an integrated modeling approach to assess changes in
21 ecosystem functions resulting from different river flow and form configurations. Moreover, it
22 investigates the role of temporal variability in such flow-form-function tradeoffs. The use of
23 synthetic, archetypal channel forms in lieu of high-resolution topographic data reduces time
24 and financial requirements, overcomes site-specific topographic features, and allows for
25 evaluation of any morphological structure of interest. In an application to California's
26 Mediterranean-montane streams, the interacting roles of channel form, water year type, and
27 hydrologic impairment were evaluated across a suite of ecosystem functions related to
28 hydrogeomorphic processes and aquatic habitat. Channel form acted as the dominant control
29 on hydrogeomorphic processes, while water year type controlled salmonid habitat functions.
30 Streamflow alteration for hydropower increased redd dewatering risk and altered aquatic
31 habitat availability. Study results highlight critical tradeoffs in ecosystem function
32 performance and emphasize the significance of spatiotemporal diversity of flow and form at
33 multiple scales for maintaining river ecosystem integrity. The proposed approach is broadly
34 applicable and extensible to other systems and ecosystem functions, where findings can be
35 used to inform river management and design testing.

37 1 Introduction

38 Rivers are complex, dynamic systems that support many natural ecosystem functions,
39 including hydrogeomorphic processes and the creation and maintenance of aquatic and riparian
40 habitat (Doyle et al. 2005). The extent and timing of these functions is largely controlled by the
41 interplay of *flow*, described by streamflow magnitude, timing, duration, frequency, and rate-of-
42 change (Poff 1997), and *form*, described by the shape and composition of the river corridor
43 (Small et al. 2008; Pasternack et al. 2008; Worthington et al. 2014; Wohl et al. 2015; Vanzo et
44 al. 2016). In spite of this complex interplay, most environmental river management studies
45 evaluate the role of either flow or form without regard for these interactions.

46 The few studies that have effectively examined flow - form interactions related to ecosystem
47 functions highlight the scientific and management value of such analyses. For instance, by
48 evaluating the potential for shallow water habitat in both the historic and current lower Missouri
49 River under alternative flow regimes, Jacobson and Galat (2006) informed restoration priorities
50 for the river. However, this and similar studies (Brown and Pasternack 2008; Price et al. 2013;
51 Gostner, Parasiewicz, et al. 2013) are site specific, limiting their applicability to the range of
52 flow and form settings exhibited by a given hydroscape, each combination supporting distinct
53 ecosystem functions. Vanzo et al. (2016) offer an exception in their evaluation of ecohydraulic
54 responses to hydropeaking over a spectrum of existing and proposed flows and forms. See

55 Supplementary materials section 1 for more details on the flow-form-function conceptual
56 framework.

57 Utilizing archetypal channel forms in lieu of detailed, site-specific datasets allows for the
58 evaluation of a larger range of flow-form settings with limited data and financial requirements.
59 An archetype refers to a simple example exhibiting typical qualities of a particular group without
60 the full local variability distinguishing members of the same group (Cullum et al. 2017). An
61 archetype-based analysis of the Yuba River, California, was employed by Escobar-Arias and
62 Pasternack (2011), who evaluated salmonid habitat conditions across archetypal 1D cross-
63 sections. An emerging technique for synthesizing digital terrain models (DTMs) of river
64 corridors using mathematical functions (Brown et al. 2014) provides an opportunity to expand on
65 the work of Escobar-Arias and Pasternack (2011) to evaluate 2D hydraulic response across any
66 channel or floodplain morphology of interest without a major increase in data requirements.

67 The application of synthetic DTMs to the evaluation of river ecosystem performance
68 bypasses data constraints of previous studies through the ability to directly generate
69 representations of historic, existing, or proposed morphologies with user-defined geomorphic
70 attributes. Synthetic river corridors have been used to evaluate controls on riffle-pool salmonid
71 habitat quality and erosion potential as well as to test the occurrence of the hydrogeomorphic
72 mechanism of flow convergence routing across a range of archetypal morphologies (Brown et al.
73 2015), but have not yet been applied to the development of ecohydraulic design criteria. At the
74 rapid rate of river habitat change and biodiversity loss (Magilligan and Nislow 2005), the ability
75 to design and compare the ecohydraulic performance of distinct morphologies with relevance
76 beyond an individual study site to an entire watershed or region would offer a powerful tool to
77 support the design of functional large-scale river rehabilitation measures.

78

79 **1.1 Study objectives**

80 This study applied synthetic DTMs of archetypal river morphologies, developed at the
81 regional scale based on an existing channel classification, to the evaluation of regional flow-
82 form-function linkages. The authors investigate the common notions of flow- and form-process
83 linkages, in which different flow regimes and morphologies are assumed to support distinct
84 hydrogeomorphic processes (Montgomery 1997; Poff 1997; Kasprak et al. 2016). The overall
85 goal of the study is to test whether archetypal combinations of flow and form attributes generate
86 quantifiable hydraulic patterns that support distinct ecosystem functions. The study objectives
87 are to (1) generate synthetic DTMs of distinct river corridor archetypes mindful of patterns of
88 topographic variability necessary to ecogeomorphic dynamics, (2) evaluate the spatiotemporal
89 patterns of depth and velocity across the archetypal DTMs from objective one, and (3) quantify
90 the performance of a suite of critical ecosystem functions across alternative flow-form scenarios.
91 The specific scientific questions addressed through these objectives are as follows: (i) Do

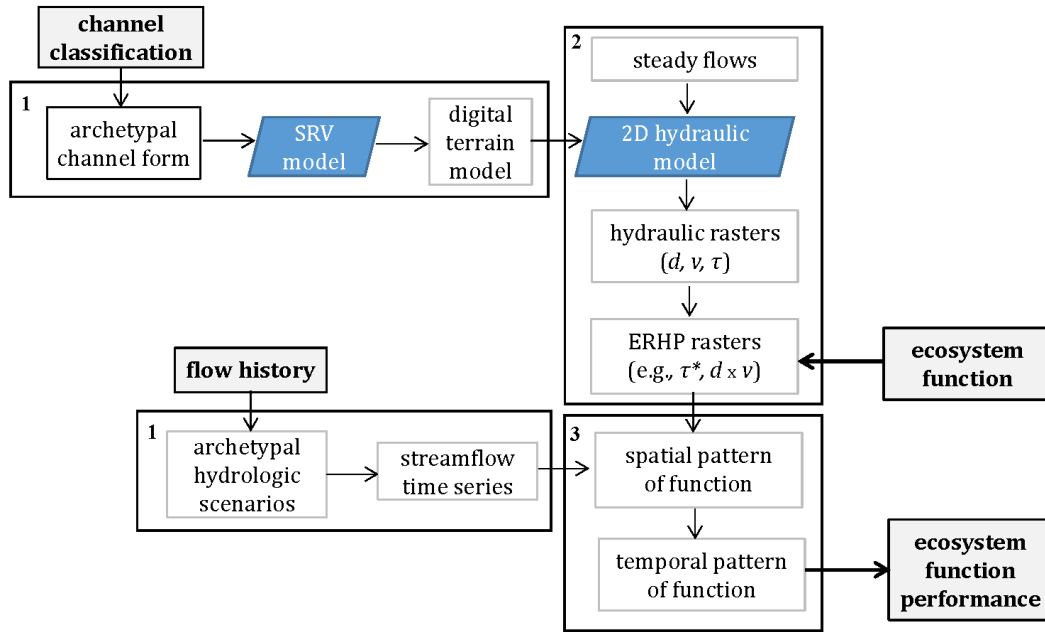
92 archetypal river corridor morphologies support distinct ecosystem functions or is more or
93 different local topographic variation within archetypes needed? (ii) What is the significance of
94 subreach-scale topographic variability in river ecosystem functioning? (iii) What is the role of
95 water year type and hydrologic impairment? (iv) What ecosystem performance tradeoffs can be
96 identified with relevance for environmental water management?

97 **1.2 Case study setting: Mediterranean-montane rivers**

98 Mediterranean-montane river systems, which exhibit cold wet winters and warm dry
99 summers, provide a useful setting for evaluating flow-form interactions because they exhibit
100 significant variability to test system sensitivity to different drivers (Gasith and Resh 1999). In the
101 California Sierra Nevada, USA, native aquatic and riparian species are adapted to the biotic
102 stresses (e.g., reduced water quality in summer) and abiotic stresses (e.g., high shear stress
103 during winter floods) associated with the highly seasonal flow regimes that depend on flow-form
104 interactions. Salmonid eggs, for example, require sufficient inundation depths and intragravel
105 flows in certain channel locations during biologically significant periods to survive (USFWS
106 2010a). Sierra Nevada rivers have been highly altered by dams and reservoir operations for water
107 supply, flood control, and hydropower (Hanak et al. 2011), driving dramatic declines in native
108 aquatic populations (Yoshiyama et al. 1998; Moyle and Randall 1998; Yarnell et al. 2012). See
109 Supplementary materials section 1.2 for more details.

110 **2 Methods**

111 The methodology can be summarized by three steps (Figure 1). First, a set of synthetic river
112 corridor DTMs is generated to represent channel types from an existing channel classification
113 (Section 2.1) and a set of hydrologic scenarios is selected for evaluation (Section 2.2). Next, a
114 2D hydrodynamic model [SRH-2D (Lai 2008)] is used to simulate ecologically relevant
115 hydraulic parameters [ERHPs, *sensu* Vanzo et al. (2016)] for each flow-form scenario (Section
116 2.3, 2.4). Finally, spatiotemporal patterns in ERHPs are used to evaluate the performance or
117 occurrence of a suite of ecosystem functions (Section 2.5) under each scenario. Each of these
118 steps is described in depth in the following paragraphs.



119
 120 Figure 1. Major steps used to quantify ecosystem function performance across archetypal channel forms
 121 and hydrologic scenarios, with step numbers associated with text above. Key inputs and outputs are
 122 bolded and modeling tools are blue parallelograms.

123 Specifically, selected streamflow time series (flows) and river corridor DTMs (forms) are
 124 input to a 2D hydrodynamic model to produce a continuum of hydraulic rasters [i.e., depth (d),
 125 velocity (v), shear stress (τ)] for a modeled river corridor at each modeled flow stage. For each
 126 model run, a set of ERHP rasters [e.g., Shields stress (τ_o^*)], indices incorporating both depth and
 127 velocity ($d \cdot v$)] is calculated from hydraulic model raster outputs. Finally, spatial and temporal
 128 statistics characterizing ERHP outputs are used first to evaluate model results in terms of depth
 129 and velocity at baseflow (0.2 x bankfull), 50% exceedance, and bankfull flows, and then to
 130 quantify the performance of distinct ecosystem functions. Bankfull discharge, defined as the flow
 131 that just reaches the transition between the channel and its floodplain, was estimated from the
 132 channel geometry as described in Section 2.4. Temporal dynamics are evaluated by integrating
 133 ERHP spatial statistics over each hydrologic scenario (Parasiewicz 2007) such that not only the
 134 magnitude but also the timing, duration, and frequency of ecosystem functions can be evaluated
 135 depending on the particular temporal requirements. The resulting annual time series represent the
 136 temporal pattern of the 2D hydraulic response in a specific DTM for a single hydrologic
 137 scenario. This process is detailed in Supplementary materials section 2.

138 The experimental design involved a series of 16 hydraulic model runs under steady flow
 139 conditions, simulating two river corridor morphologies across eight discharges spanning
 140 baseflow (0.2x bankfull) to twice bankfull flow stages. The decision to evaluate proportions of
 141 bankfull flow was driven by the established geomorphic and ecological significance of bankfull
 142 flow in the literature (Wolman and Miller 1960; Doyle et al. 2005; Richter and Richter 2000).
 143 Further, scaling flows by a common non-dimensional metric allows for readers worldwide to

144 evaluate these results relative to the setting in their locality. These eight discharges discretized
145 the daily flow regimes evaluated to simplify temporal analysis. All simulated combinations were
146 designed to reproduce realistic archetypal flow and form conditions in Mediterranean-montane
147 river systems for two channel types of interest, plane bed and pool-riffle (see section 2.1). A
148 rigorous scaling approach to compare the full range of possible configurations was outside the
149 scope of the current study. The following sections describe the flow regimes, river corridor
150 morphologies, hydraulic modeling approach, and ecosystem functions considered.

151 **2.1 Synthetic river corridor morphologies**

152 Two archetypal river corridor morphologies distinguished in the Sacramento Basin channel
153 classification by Lane, Pasternack, et al. (2017) were considered in this study as a proof-of-
154 concept: semi-confined plane bed and semi-confined pool-riffle. These morphologies were
155 selected for their common occurrence in mid-elevation montane environments (Montgomery and
156 Buffington 1997; Wohl and Merritt 2005) and their similar channel dimensions and slopes
157 contrasted by major differences in subreach-scale topographic variability. An existing field data
158 driven channel classification for the Sacramento Basin (Lane, Pasternack, et al. 2017) provided
159 the parameter values needed to synthesize the two archetypal morphologies, quantified as the
160 median field-surveyed values for each channel type.

161 DTMs of the investigated channel types were generated using the synthetic rivers model
162 developed by Brown et al. (2014). Below, we briefly provide the equations vital to understanding
163 the DTMs created in this study. The goal of the design process was to capture the essential
164 organized features of each channel type so that their functionalities can be evaluated in a
165 reductionist approach without the random details of real river corridors that cause highly
166 localized effects.

167 **2.1.1 Reach-average parameters**

168 The synthetic rivers approach first creates a reach-averaged river corridor that is scaled by
169 reach-averaged bankfull width (w_{BF}) and bankfull depth (h_{BF}), with median sediment size (D_{50}),
170 slope (S), sinuosity, and floodplain width and lateral slope as user-defined input variables. For
171 each synthetic river scenario, 140 longitudinal nodes were spaced at 1 m ($\sim 1/10$ bankfull channel
172 widths).

173 **2.1.2 Channel variability functions**

174 Next, this approach incorporates subreach-scale (<10 channel widths frequency) topographic
175 variability because many hydrogeomorphic processes of ecological significance depend on
176 specific patterns of topographic variability and associated habitat heterogeneity (MacWilliams et
177 al. 2006; Poff and Ward 1990; Scown et al. 2015). The local bankfull width at each location x_i
178 along the channel, $w_{BF}(x_i)$, is given by Eq. 1 as a function of reach-averaged bankfull width w_{BF}

179 and a variability control function $f(x_i)$, with a similar equation used to characterize vertical bed
180 undulation that incorporates S :

$$181 \quad w_{BF}(x_i) = w_{BF} * f(x_i) + w_{BF} \quad [1]$$

182 There are many available mathematical and statistical control functions that may be used to
183 describe archetypal river variability (Brown and Pasternack 2016). For this study, the variability
184 of w_{BF} and h_{BF} about the reach-averaged values was determined by a sinusoidal function, as

$$185 \quad f(x_i) = a_s \sin(b_s x_r + h_s) \quad [2]$$

186 where a_s , b_s , and h_s are the amplitude, angular frequency, and phase shift alignment parameters
187 for the sinusoidal component, respectively, and x_r is the Cartesian stationing in radians. The
188 Cartesian stationing was scaled by w_{BF} so that the actual distance was given by $x_i = x_r * w_{BF}$.
189 The sinusoidal function alignment parameters were adjusted iteratively to achieve desired values
190 for h_{BF} , width-to-depth ratio (w/h_{BF}), sinuosity, and the coefficient of variation (CV) of w_{BF}
191 and h_{BF} based on plane bed and pool-riffle channel classification archetypes (Lane, Pasternack,
192 et al. 2017). Floodplain confinement, the bankfull to floodplain width ratio, was used to set
193 valley width and overbank topography.

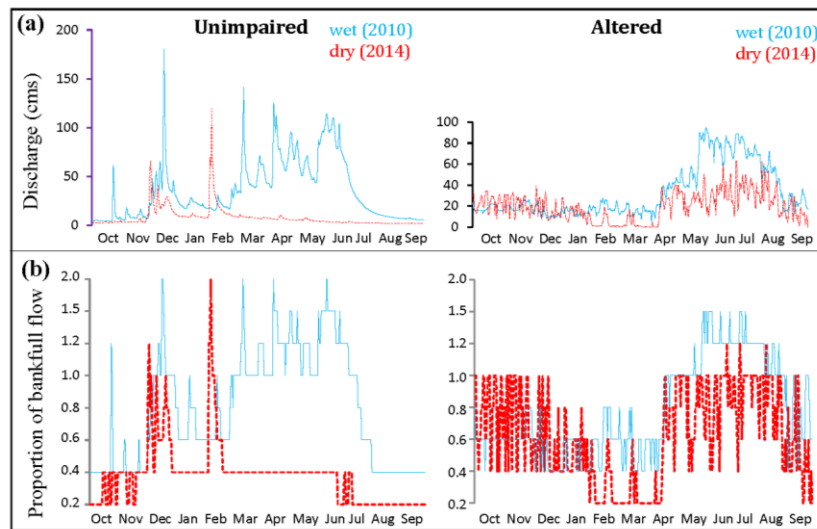
194 Because river classifications traditionally aim to capture the central tendency of river types at
195 the reach scale, they contain little to no information on subreach-scale topographic variability
196 and landform patterning (Lane, Pasternack, et al. 2017). This study used outputs from a channel
197 classification that was unique in including statistical characterization of subreach width and
198 depth variability using the metric of CV, based on the average and standard deviation of field-
199 derived values (Lane, Pasternack, et al. 2017). However, there remained numerous landform
200 patterning permutations using the control function parameters of Eq. 2 that could yield those CV
201 values, many associated with profoundly different geomorphic processes. In these cases, field
202 experience and judgment informed the design of topographies capable of supporting the
203 dominant geomorphic processes of each channel type as outlined in the classification study. For
204 example, for the pool-riffle system, minimum depth and maximum width were made to
205 positively covary in the DTM to represent this patterning (Brown and Pasternack 2016).

206

207 **2.2 Flow regimes**

208 Four hydrologic scenarios characteristic of the mixed snowmelt and rain flow regime typical
209 of Mediterranean-montane systems were evaluated (Lane, Dahlke, et al. 2017): unimpaired wet,
210 unimpaired dry, altered wet, and altered dry annual flow regimes (Figure 2). Daily streamflow
211 time series for two mid-elevation gauge stations in the western Sierra Nevada, California, were
212 chosen to represent these archetypal flow regimes under unimpaired (North Yuba River below
213 Goodyears Bar) and altered (New Colgate Powerhouse) conditions (see Supplementary materials

214 section 2.2 for map of gage locations). These gauges lie within similar physioclimatic and
 215 geologic settings and provide daily streamflow time series for both an extremely wet (WY 2010;
 216 >75th percentile annual streamflow) and an extremely dry (WY 2014; <25th percentile annual
 217 streamflow) water year. The New Colgate Powerhouse gage captures typical hydropeaking
 218 patterns of Sierra Nevada streams. The 50% exceedance flows for each hydrologic scenario are
 219 23.3, 5.0, 19.2, and 18.5 m³/s for the wet unimpaired, dry unimpaired, wet altered, and dry
 220 altered scenarios, respectively.



221
 222 Figure 2. Four hydrologic scenarios were considered: unimpaired wet, unimpaired dry, altered wet, and
 223 altered dry. Graphs illustrate unimpaired and altered daily time series of (a) streamflow and (b)
 224 discretized proportions of bankfull flow based on stage-discharge thresholds from Table 1.

225

226 2.3 Hydraulic modeling

227 The surface-water modeling system (SMS; Aquaveo, LLC, Provo, UT) user interface and
 228 Sedimentation and River Hydraulics- Two Dimensional (SRH-2D) algorithm (Lai 2008) were
 229 used to produce exploratory hydrodynamic models for each flow-form scenario. SRH-2D is a
 230 finite-volume numerical model that solves the Saint Venant equations for the spatial distribution
 231 of water surface elevation, water depth, velocity, and bed shear stress at each computational
 232 node. It can handle wetting/drying and supercritical flows, among other features. The parametric
 233 eddy viscosity equation was used for turbulence closure. A coefficient value of 0.1 suitable for
 234 shallow rivers with coarse bed sediment was used in that equation. A computational mesh with
 235 internodal mesh spacing of 1 m (relative to a channel width of 10 m) was generated for each
 236 synthetic DTM. Because this study was purely exploratory, using numerical models of
 237 theoretical river archetypes, no calibration of bed roughness or eddy viscosity was possible.
 238 Similarly, no validation of model results was possible.

239 The model required inputs of discharge and downstream flow stage as well as boundary
 240 conditions of bed topography and roughness. Eight model runs for each morphology capture the
 241 discharge range of 0.2 - 2.0 x bankfull flow stage (Table 1), where bankfull flow stage is the
 242 water surface elevation at which flows spill onto the floodplain. The specific simulated discharge
 243 values associated with these stages were estimated for each morphology using Manning's
 244 equation based on representative cross-sections of the synthetic DTMs. Bankfull stage and
 245 wetted perimeter were determined manually from the cross-sections, and cross-sectional area
 246 was calculated using the trapezoidal approximation. Manning's n was set at 0.04 to represent a
 247 typical unvegetated gravel/cobble surface roughness (Abu-Aly et al. 2014).

248 Table 1. Simulated channel archetype discharge values for 0.2 - 2.0 times bankfull flow stage
 249 calculated from Manning's equation, and associated stage - discharge threshold estimates for the North
 250 Yuba River.

Fraction of bankfull flow	Simulated discharge		N. Yuba River discharge
	Plane Bed (m ³ /s)	Pool-Riffle (m ³ /s)	Stage - discharge threshold (m ³ /s)
0.2	1.3	1.2	2.8
0.4	6.8	4.5	14.2
0.6	17.7	9.7	22.7
0.8	28.7	17.8	28.3
1.0	58.2	27.7	56.6
1.2	95.5	64.3	85.0
1.5	164.4	139.9	113.3
2.0	310.3	338.1	141.6

251

252 2.4 Hydrological scaling

253 Finally, in order to scale the real streamflow time series to the synthetic DTMs, stage -
 254 discharge relationships are needed to associate each of the eight flow stages simulated in the
 255 hydraulic model (Table 1) with the actual discharge required to fill the North Fork Yuba river
 256 channel to that flow stage. In the absence of local stage-discharge relationships, these thresholds
 257 were instead estimated manually (Table 1, final column) with the aim of retaining archetypal
 258 hydrologic characteristics of interest. Specifically, stage thresholds were set so, in the wet year,
 259 the flow stage time series remained at or above bankfull during winter storms and throughout the
 260 spring snowmelt recession while, in the dry year, flow stage rarely exceeded bankfull and spent
 261 the majority of summer at base flow. The estimated stage - discharge thresholds were justified by
 262 the ability of the discretized flow regimes (Figure 2b) to retain these hydrologic patterns
 263 exhibited by the un-discretized flow regimes (Figure 2a). However, these thresholds are
 264 estimates and should not be considered as ultimate targets to inform river management. A major
 265 assumption of this approach is that the flow stage discretization captures all significant spatial
 266 hydraulic patterns in the river corridor relative to the functions under consideration in this study
 267 (see Supplementary materials for more details).

268 **2.5 River ecosystem functions**

269 Five Mediterranean-montane ecosystem functions were considered, associated with two
 270 major components of river ecosystem integrity: hydrogeomorphic processes and aquatic habitat
 271 (Table 2). The performance of these functions was tested based on the following criteria: (1) a
 272 longitudinal shift in the location of peak shear stress at high flows from topographic highs to
 273 topographic lows was used to test the occurrence of flow convergence routing, a dominant
 274 geomorphic formation and maintenance process in certain channels (MacWilliams et al. 2006);
 275 (2) a measure of hydrogeomorphic variability was used to quantify overall habitat heterogeneity
 276 in the river corridor (Gostner, Alp, et al. 2013); and (3) fall-run Chinook salmon habitat was
 277 evaluated with respect to (a) bed preparation and (b) bed occupation functions based on
 278 established shear stress thresholds and biologically significant timing thresholds (Escobar-Arias
 279 and Pasternack 2010) as well as (c) redd dewatering risk during bed occupation. These functions
 280 were evaluated using a Python script that enabled rapid evaluation of model outputs over the
 281 specific spatio-temporal constraints.

282 Table 1. The five river ecosystem functions evaluated in this study and their associated ecologically
 283 relevant hydraulic parameters (ERHPs), biologically relevant periods, and spatial extents.

Ecosystem Function	ERHP(s)	Biological Period	Spatial Extent	Citations
Hydrogeomorphic processes				
Flow convergence routing	shear stress	--	bankfull channel	MacWilliams et al. 2006
Hydrogeomorphic diversity	velocity, depth	--	river corridor	Gostner et al. 2013a
Aquatic habitat				
Salmonid bed preparation	shear stress	Oct – Mar	bankfull channel	Escobar-Arias and Pasternack 2010
Salmonid bed occupation	shear stress	Apr – Sep	bankfull channel	
Redd dewatering	velocity, depth	Oct – Mar	spawning channel	USFWS, 2010b

284 **2.5.1 Flow convergence routing mechanism**

285 Flow convergence routing, the periodic reversal of peak shear stress location, is often
 286 considered critical to pool-riffle maintenance (White et al. 2010). The Caamaño criterion
 287 (Caamaño et al. 2009) was used to estimate the minimum riffle depth needed for a reversal to
 288 occur in each archetypal morphology. This mechanism was further evaluated based on the
 289 presence of a shift in peak shear stress from topographic wide-highs (riffles) to narrow-lows
 290 (pools), which indicates that the locations of scour and deposition are periodically shifted in the
 291 channel to maintain the relief between riffles and pools (Brown and Pasternack 2014).

292 **2.5.2 Hydrogeomorphic diversity**

293 The hydro-morphological index of diversity (HMID) (Gostner, Alp, et al. 2013) was used to
 294 quantify overall physical heterogeneity of the river corridor as follows, where the coefficient of
 295 variation (CV) is the standard deviation of depth or velocity divided by its mean:

296
$$HMID_{reach} = (1 + CV_v)^2 * (1 + CV_d)^2 \quad [3]$$

297 Three tiers of HMID were delineated as follows: HMID <5 indicates simple uniform or
 298 channelized reaches; 5 < HMID <9 indicates a transitional range from uniform to variable
 299 reaches; HMID >9 indicates morphologically complex reaches (Gostner, Parasiewicz, et al.
 300 2013). To date, no studies have applied this index to archetypal terrains, so this is a novel
 301 application to further understand its value in quantifying ecosystem functions. Percent
 302 exceedance curves of HMID provided graphical representations of the temporal patterns of
 303 hydraulic diversity under alternative flow-form scenarios.

304 **2.5.3 Salmonid bed occupation and preparation**

305 Ecosystem functions related to salmonid habitat can be split into bed occupation functions,
 306 which occur while the fish are directly interacting with the channel bed (i.e. spawning,
 307 incubation and emergence), and (2) bed preparation functions, which occur between occupation
 308 periods during migration (Escobar-Arias and Pasternack 2011). A stable bed, indicated by low
 309 shear stress ($\tau_o^* < \tau_{c50}$), is needed to minimize scour during bed occupation (Oct – Mar), while
 310 high shear stress capable of mobilizing the active layer ($\tau_o^* > \tau_{c50}$) is necessary to rejuvenate the
 311 sediment during bed preparation (Apr – Sep) (Soulsby et al. 2001; Konrad et al. 2002). See
 312 Supplementary materials section 2.5.4 for more details.

313 Bed mobility transport stages delimited per-pixel by nondimensional boundary shear stress or
 314 Shields stress (τ_o^*) thresholds (Jackson et al. 2015) were used to quantify these bed occupation
 315 and preparation functions according to the following equation:

316
$$\tau_o^* = \frac{\tau_b}{g(\rho_s - \rho)D_{50}} \quad [4]$$

317 where τ_b is bed shear stress:

318
$$\tau_b = \rho_w (u^*)^2 \quad [5]$$

319 based on water density (ρ_w) and shear velocity $u^* = U\sqrt{C_d}$, where U is depth-averaged velocity
 320 for an individual pixel and C_d is the depth-based drag coefficient (Pasternack 2011). τ_o^* therefore
 321 varies spatially and with discharge as a function of depth and velocity. For the present
 322 application, a stable bed is assumed when $\tau_o^* < 0.01$, intermittent transport when $0.01 < \tau_o^* < 0.03$,
 323 partial transport when $0.03 < \tau_o^* < 0.06$ and full mobility when $0.06 < \tau_o^* < 0.10$ (Buffington and
 324 Montgomery 1997). At each discharge, the areal proportion of each bed mobility tier occurring
 325 in the river corridor region of interest can be calculated. Function performance is then quantified
 326 through time as the cumulative proportion of the channel providing functional bed mobility
 327 conditions during biologically relevant periods. Results are then binned such that low, mid, and
 328 high performances are associated with 0-25%, 25-75%, and 75-100% performance. For example,
 329 at least 75% of the channel area must exhibit partial or full bed mobility on average over the bed
 330 preparation period to achieve high bed preparation performance.

331 **2.5.4 Redd dewatering**

332 Salmonid redd dewatering is a major concern in Sierra Nevada streams managed for
333 hydropower (USFWS 2010b). Reductions in flow stage exposing the tailspill and reductions in
334 velocity diminishing intragravel flow through the redd can dramatically reduce the survival of
335 salmonid eggs and pre-emergent fry (Healey 1991; USFWS 2010b). This study focused on fall-
336 run Chinook salmon (*Oncorhynchus tshawytscha*) as an important species in Sierra Nevada
337 streams. Redd dewatering risk was measured as the areal proportion of viable spawning habitat
338 with depth below 0.15 m and/or velocity below 0.09 m/s during the occupation period
339 [incubation and emergence period (Dec – Mar) (USFWS 2010b)]. Viable spawning habitat was
340 defined according to USFWS as the portion of the bankfull channel with velocity from 0.1 - 1.6
341 m/s and depth from 0.15 - 1.3 m at 0.4x bankfull stage, the most common stage experienced
342 under unimpaired conditions during the spawning period (Oct – Dec) (USFWS 2010a).

343 **2.6 Holistic ecosystem functions analysis**

344 There is limited guidance available in the literature regarding how best to evaluate and
345 visually represent the environmental performance of rivers across a suite of ecosystem functions.
346 The question of how best to evaluate environmental performance using individual metrics or
347 functions is well established (CITE). The broader water resources management literature offers
348 several summary performance indices that could be applied to this new setting. For example, the
349 water resources management sustainability index (Sandoval-Solis et al. 2010), which evaluates
350 different water management policies by summarizing across metrics of reliability, resilience, and
351 vulnerability, could be applied as a summary index of environmental performance. In this study,
352 we created a graphic that aligns all of the ecosystem functions in one table to visualize the
353 performance of a suite of temporally varying functions simultaneously.

354 **3 Results**

355 The synthetic DTM results are presented first (study objective 1). Then the hydraulic
356 modeling results are discussed in terms of depth and velocity patterns (study objective 2).
357 Finally, model results are used to interpret the performance of five ecosystem functions (Table 2)
358 across alternative flow-form scenarios (study objective 3).

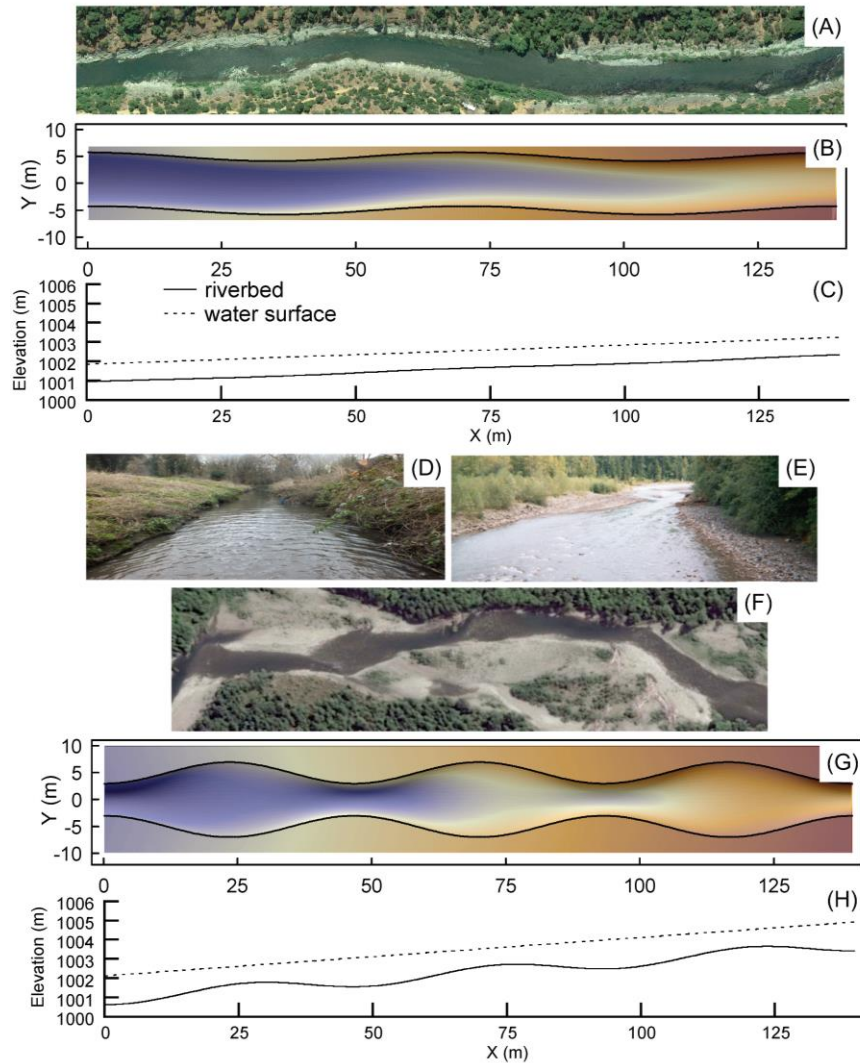
359 **3.1 Synthetic digital terrain models**

360 Two 140 m long synthetic DTMs were generated representing archetypal morphological
361 configurations of semi-confined pool-riffle and plane bed morphologies (Figure 3). These DTMs
362 exhibited distinct reach-averaged attributes (e.g., S , w/h_{BF} , and D_{50}) (Table 3a), subreach-scale
363 topographic variability (e.g., CV), and proportions of the river corridor exhibiting positive and
364 negative geomorphic covariance structures (GCSs) (Table 3b). The sinusoidal function
365 alignment parameters used are listed in Table 3b. The resulting morphologies exhibited major
366 differences in subreach-scale topographic variability as illustrated by the planform and

367 longitudinal topographic patterns in Figure 3. The bankfull channel area was 868 m² in the pool-
 368 riffle and 1,041 m² in the plane bed DTM.

369 Table 2. (a) Channel and floodplain geomorphic attributes and (b) control function alignment
 370 parameters used in the design of synthetic DTMs of plane bed and pool-riffle channel morphologies

(a) Geomorphic Attributes			(b) Alignment Parameters		
Plane Bed			Pool - Riffle		
Channel			Planform		
w _{BF} (m)	10	10	phase shift	0	0
h _{BF} (m)	1	1	amplitude	0.8	0
S (%)	1	2	frequency	2	2
w/h _{BF}	10	10	Bankfull Width		
D ₅₀ (m)	0.2	0.1	phase shift	$\pi/2$	π
sinuosity	1.1	1.1	amplitude	0.01	0.5
CV _{w_{BF}}	0.01	0.35	frequency	2	3
CV _{H_{BF}}	0.03	0.18	Bed Elevation		
+ GCS (%)	55	86	phase shift	0	2.7
- GCS (%)	45	14	amplitude	0.04	0.35
Floodplain			frequency	2	3
confinement	0.5	0.5	Floodplain Outline		
lateral slope	0.80%	0.80%	phase shift	0	0
width (m)	16	16	amplitude	0	0.5
D ₅₀ (m)	0.03	0.03	frequency	1.5	1.5



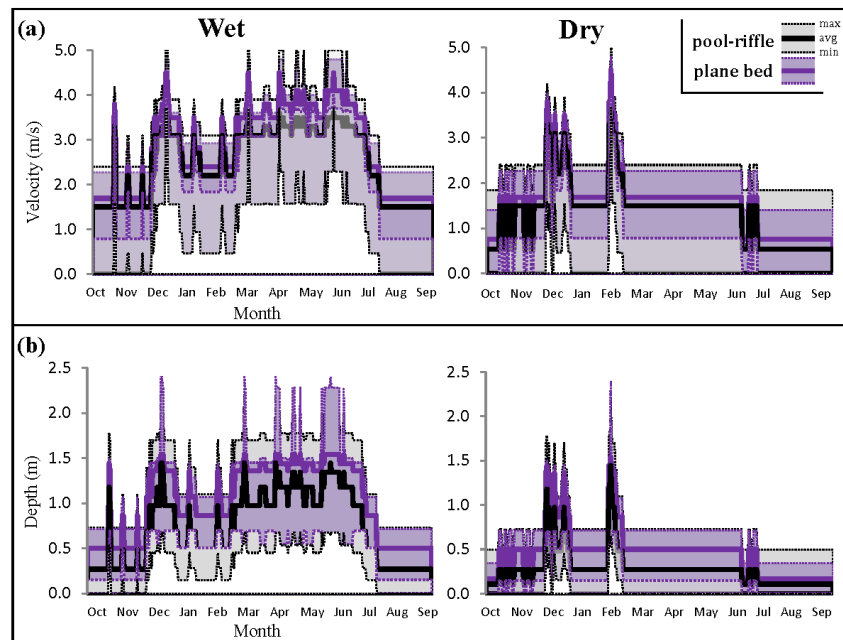
371
 372 Figure 3. Two archetypal river corridor morphologies were evaluated, plane bed (A - D) and pool-riffle (E
 373 - H). The synthetic DTMs (B and G) are shown overlaid by their bankfull channel boundaries, where dark
 374 red is high elevation and dark blue is low elevation, followed by their longitudinal profiles (C and H).

375 3.2 Spatial and temporal distribution of hydraulic variables

376 Depth and velocity values fell within typical ranges for gravel-bed montane streams across
 377 base, 50% exceedance, and bankfull flows, supporting the archetypal specifications used in this
 378 study (Richards 1976; Jowett 1993). Water depths ranged from 0.0 to 2.4 m, with higher average
 379 depths in the plane bed than the pool-riffle across all three flows. The pool-riffle had lower
 380 minimum and higher maximum depths across all flow levels, resulting in a larger depth range
 381 and CV. Flow velocities ranged from 0.0 to 5.5 m/s, exhibiting a similar pattern to depth between
 382 morphologies, with higher average and minimum velocities in the plane bed across all 8
 383 discharge stages. In contrast with depth, however, at bankfull flow maximum velocity was
 384 significantly higher in the plane bed than the pool-riffle, resulting in a higher velocity CV. The

385 HMID was substantially higher at base flow than higher flows, and was more than twice as high
386 in the pool-riffle as in the plane bed at base flow.

387 Time series plots of hydraulic summary statistics illustrate the daily temporal variability of
388 depth and velocity over the four hydrologic scenarios (Figure 4). A reversal in the maximum CV
389 of velocity from the pool-riffle to the plane bed is evident during spring in the wet unimpaired
390 scenario and during summer in the wet altered scenario, corresponding with a very high
391 maximum velocity in the plane bed (5.5 m/s). The remainder of seasons and water year types
392 exhibit higher hydraulic variability in the pool-riffle, with the largest differences in CV occurring
393 at low flows.



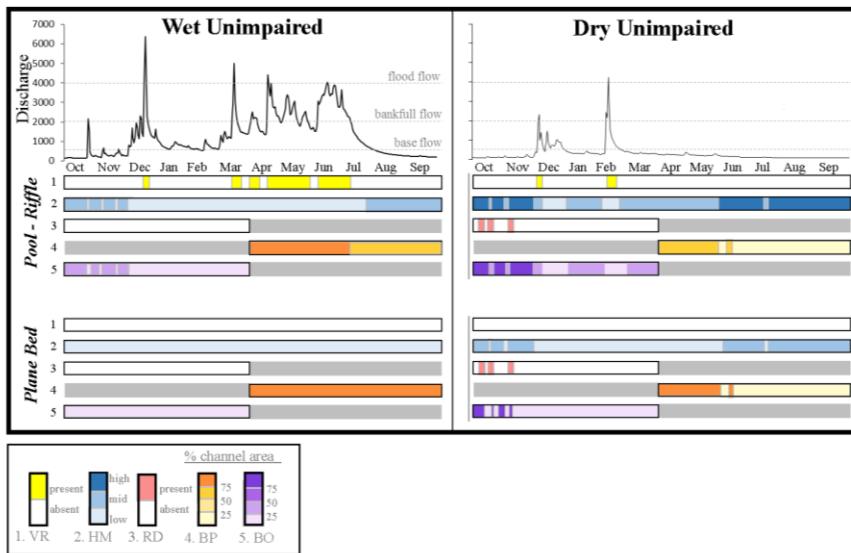
394
395 Figure 4. Annual time series plots of maximum, average, and minimum (a) flow velocity and (b) water
396 depth in plane bed and pool-riffle morphologies over four hydrologic scenarios.

397 Water depth was more sensitive to low flow variations in terms of rate of change, while
398 velocity was more sensitive to changes in high flows. This likely occurs because, in parabolic
399 channel geometries, the channel fills rapidly from low to bankfull flow, whereas, once the
400 bankfull channel is overtopped, a larger flow increase is required to engender the same increase
401 in water depth over the wider floodplain so high flow changes translate more directly to velocity.
402 With regards to channel type, the pool-riffle morphology demonstrated an approximately linear
403 increase in depth with flow, while the plane bed morphology demonstrated a rapid increase in
404 depth from low flow to 0.8x bankfull and a reduced rate of increase at higher flows. Conversely,
405 velocity in both morphologies increased at a slow linear rate from low flow to 0.8x bankfull flow
406 and then increased much faster in the plane bed at higher flows. Only at high flows (>1.5x
407 bankfull) did pool-riffle velocity exhibit a strong sensitivity to flow variability. These findings
408 demonstrate that changes in the hydraulic environment due to variations in discharge were

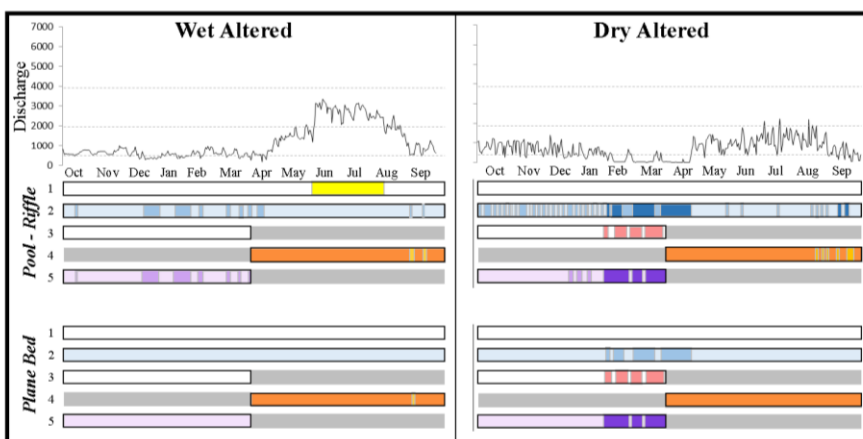
409 stronger in the plane bed than the pool-riffle, indicating that pool-riffle hydraulics are less
 410 sensitive to changes in flow on average but instead exhibit more complex spatial patterns.

411 3.3 Ecosystem function performance results

412 All six Mediterranean-montane river ecosystem functions were found to be controlled by
 413 both flow and form attributes to varying extents, as illustrated in Figure 5 for the unimpaired
 414 flow regime and in Figure 6 for the altered flow regime.



415
 416 Figure 5. Summary of temporally varying ecosystem function performance under an unimpaired flow regime
 417 across four flow-form scenarios: wet – pool-riffle, wet – plane bed, dry – pool-riffle, dry – plane bed. The five
 418 ecosystem functions evaluated are: 1. Flow convergence routing (VR), 2. hydrogeomorphic diversity (HG), 3. redd
 419 dewatering risk (RD), 4. salmonid bed preparation (BP), and 5. salmonid bed occupation (BO). Tiered performance
 420 is indicated in the key by increasingly dark shading and bimodal performance (VR and RD) is either colored or
 421 empty. Greyed regions indicate periods of the year that functions are not biologically relevant. Base flow = 0.2x,
 422 bankfull flow = 1.0x, and flood flow = 1.5x bankfull flow as defined in Table 1.



423
 424 Figure 6. Summary of temporally varying ecosystem function performance under an altered flow regime across
 425 four flow-form scenarios: wet – pool-riffle, wet – plane bed, dry – pool-riffle, dry – plane bed (key in Fig. 5).

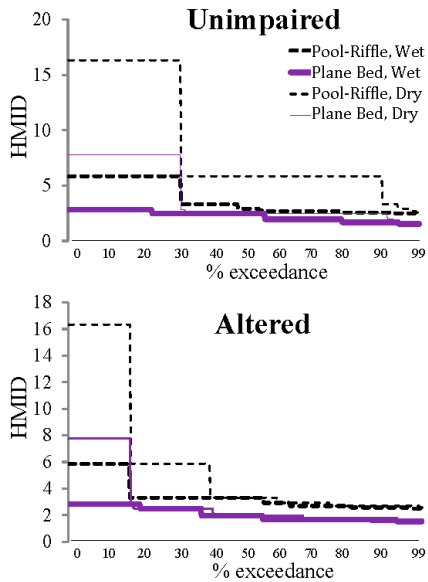
426 3.3.1 *Flow convergence routing*

427 The pool-riffle morphology demonstrated a shear stress reversal from low to high flow, as
428 indicated by a Caamaño criterion riffle depth threshold for reversal of 0.21 m (approximately
429 0.4x bankfull stage) and a shift in the location of peak shear stress from the riffle crest to the pool
430 trough from base to bankfull flow (see Supplementary materials for more details). The existence
431 of a dominant flow convergence routing mechanism is further indicated by 86% of the pool-riffle
432 morphology exhibiting a positive GCS (i.e., primarily wide shallow riffles and narrow deep
433 pools). Alternatively, the plane bed morphology did not exhibit a shear stress reversal based on
434 either the Caamaño criterion or a peak shear stress location shift, and only 55% of the river
435 corridor exhibited positive GCS.

436 3.3.2 *Hydrogeomorphic diversity (HMID)*

437 HMID was higher in the pool-riffle than the plane bed morphology at flows up to 1.2x
438 bankfull, beyond which they were nearly equivalent. That is, for a given hydrologic scenario, the
439 cumulative HMID over the year was higher in the pool-riffle. The highest index values and the
440 greatest difference between the two morphologies occurred at the lowest flow stage (0.2x
441 bankfull discharge), when HMID was twice as high in the pool-riffle. The rapid decrease in
442 HMID for in-channel flows in both morphologies with increasing discharge illustrates the limited
443 temporal persistence of high diversity hydraulic habitats in all but the lowest flow conditions. In
444 natural conditions, once flows spill over the banks, there should be a significant increase in
445 HMID as topographically heterogeneous floodplains inundate. However, in the absence of
446 detailed floodplain attributes from the channel classification, this study considered simple
447 floodplain morphologies in both archetypes.

448 HMID exceedance curves for each of the eight flow-form scenarios provided insight into
449 hydraulic diversity patterns (Figure 7). As low flows produce higher HMID values in general, it
450 is unsurprising that in a very dry year both morphologies exhibited high HMID for most of the
451 year. Under dry conditions, the unimpaired flow regime provided nearly twice as many days with
452 high HMID in both morphologies. Under the altered flow regime, HMID was slightly higher in
453 the wet pool-riffle than the dry plane bed for all flows above 17% exceedance. The highest
454 HMID was exhibited by the pool-riffle under dry unimpaired conditions (HMID=5.9),
455 presumably due to the combination of high topographic variability and extended summer low
456 flows. At the 50% exceedance flows of each hydrologic scenario, hydraulic diversity was more
457 sensitive to water year type than hydrologic alteration, and appeared to be most controlled by
458 channel morphology. Alternatively, at the 10% exceedance flows, water year type played a more
459 significant role, with the dry year exhibiting much higher HMID across both morphologies and
460 impairment conditions. More significantly, the temporal analysis of HMID revealed that, unlike
461 the dry altered flow regime, the dry unimpaired flow regime exhibited high HMID during the
462 fall-run Chinook bed occupation period, as detailed in the Supplementary materials.

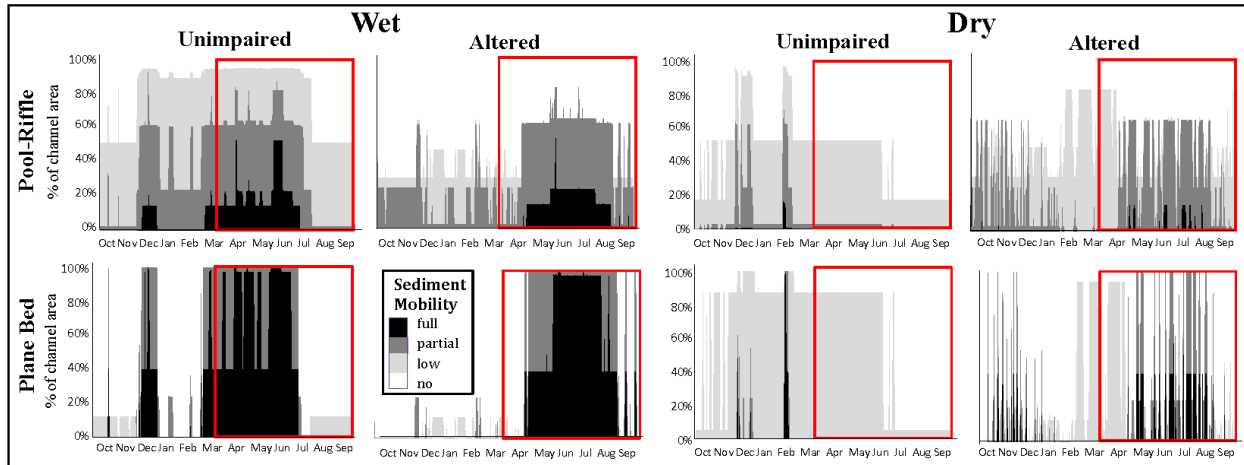


463
 464 Figure 7. Hydromorphic index of diversity (HMID) exceedance curves for (a) unimpaired and (b)
 465 altered flow regimes under different channel morphologies and water year types.

466 3.3.3 *Salmonid bed preparation and occupation*

467 Significant differences in salmonid habitat performance across flow-form scenarios were
 468 identified from shear stress based sediment mobility patterns (Figure 8). Under unimpaired
 469 conditions, the wet year exhibited high bed preparation performance and low bed occupation
 470 performance, while the dry year exhibited mid performance in both functions with reduced bed
 471 preparation but increased bed occupation performance. Under streamflow alteration, bed
 472 preparation performed well across water years while bed occupation performed poorly across
 473 water years and morphologies due to increased sediment mobility under elevated low flows
 474 during the occupation period. Spatially, in the pool-riffle channel, higher sediment mobility
 475 occurred over the riffle crests while the pools remained less mobile at all but flood flows.
 476 Conversely, sediment mobility was nearly uniform in the plane bed channel across all flows.

477



478
 479 Figure 8. Daily time series plots of the proportion of the bankfull channel exhibiting different tiers of
 480 sediment mobility illustrate the performance of salmonid bed preparation (boxed, partial/high mobility
 481 from Apr-Sep) and occupation (no/low mobility from Oct-Mar) functions.

482
 483 **3.3.4 Redd dewatering**

484 Viable spawning habitat, based on depth and velocity requirements, varied between the
 485 channel forms. Nearly 50% of the bankfull channel provided viable spawning habitat in the pool-
 486 riffle compared to only 31% in the plane bed. Pool-riffle spawning habitat was extensive and
 487 patchy, excluding only excessively high velocity zones on the riffle crests. Alternatively, plane
 488 bed spawning habitat only occurred in 1-2 meter bands along the wetted channel margins with
 489 sufficiently low velocity to meet predefined spawning requirements.

490 Redd dewatering risk within viable spawning habitat areas also varied significantly across
 491 flow-form scenarios. Redd dewatering risk was greater in the plane bed than the pool-riffle at
 492 base flow (100% vs 57% of spawning habitat) but risk was maintained across a greater range of
 493 flows (0.2 - 0.4x bankfull flow) in the pool-riffle. This is because the pool-riffle morphology has
 494 more gradual side slopes and the total available spawning habitat is greater. High dewatering risk
 495 (>30% of spawning habitat) occurred only in the dry altered scenario, with very low flows
 496 occurring throughout the redd incubation (Oct – Dec) and emergence (Jan – Mar) periods.

497
 498 **4 Discussion**

499 **4.1 The utility of synthetic river archetypes**

500 This study demonstrated the ability to synthesize DTMs from channel classification
 501 archetypes exhibiting distinct ecosystem function performance, offering a scientifically
 502 transparent, repeatable, and adjustable framework for flow-form-function inquiry. Specific

503 geomorphic attribute values were accurately represented by the synthetic morphologies,
504 including channel dimensions, cross-sectional geometry, depth and width variability, sinuosity,
505 and slope (Fig. 3). The flow convergence routing mechanism was shown to occur in the pool-
506 riffle archetype but not in the plane bed one, confirming that the two morphologies were
507 capturing distinct geomorphic maintenance processes as distinguished by the Sacramento Basin
508 channel classification (Lane, Pasternack, et al. 2017). Once a person understands how to produce
509 a synthetic DTM with the required subreach-scale variability to drive geomorphic processes and
510 ecological functions, then the software implements that very quickly. As a result, time and
511 financial requirements are dramatically reduced compared to doing a field-based campaign
512 involving meter-resolution topographic surveying, parameter calibration, and quality assurance
513 procedures. This approach therefore liberates future research to explore and isolate a larger range
514 of flow and form characteristics than those considered in the present study. This is an important
515 first step for evaluating how different kinds of rivers function, but care should be used in
516 extrapolating the specific results to any specific actual channel topography for real river
517 management. Archetypal studies provide useful guidelines, and then local studies should be
518 conducted to ascertain how the mechanisms play out in their details in the local setting, possibly
519 including validation efforts, to the extent feasible.

520 To choose the correct permutation of depth and width parameters to the synthetic
521 morphologies, expert judgment was used based on field experience and understanding of how to
522 interpret the processes associated with different patterns of topographic variability. However,
523 some attributes required to generate representative topographic attributes, such as floodplain
524 width variability and floodplain lateral slope, were not available in the channel classification of
525 Lane, Pasternack, et al. (2017). This represents an important limitation of the proposed method,
526 because useful results for certain ecosystem functions (e.g., riparian recruitment) require better
527 information than is currently available. More datasets focusing on different aspects of
528 geomorphic variability at different scales would enable more informed metric and parameter
529 choices (Brown and Pasternack 2017).

530 **4.2 Ecological significance of specific patterns of topographic variability**

531 The spatial and temporal distributions of depth and velocity across channel forms illustrate
532 differences in sensitivity to flow changes, with major implications for ecosystem functioning and
533 aquatic biodiversity (Dyer and Thoms 2006). The pool-riffle morphology was less sensitive to
534 temporal changes in flow in terms of associated changes in depth and velocity, but more spatially
535 variable, exhibiting a larger range and CV of depth and velocity values for a given discharge.
536 This indicates that the pool-riffle has more sustained persistence of hydraulic patterns, making
537 many ecosystem functions less prone to temporal fluctuations with flow as long as the discharges
538 fall below the threshold for particular processes (Gostner, Parasiewicz, et al. 2013).

539 Study results support emerging scientific understanding that many river ecosystem functions
540 are controlled by subreach-scale topographic variability (White et al. 2010; Brown and

541 Pasternack 2016; Thompson 1986; Murray et al. 2006) by quantifying the occurrence of distinct
542 ecosystem functions in reaches of high versus low topographic variability. Specifically, results
543 emphasize that it is not enough to just obtain random topographic variability or any arbitrary
544 coherent permutation of variability, but rather the pattern of organized variability must meet the
545 requirements of the appropriate GCS and dominant geomorphic processes for that channel
546 archetype (Brown and Pasternack 2014; Brown et al. 2015).

547 Distinct spatial and temporal hydraulic patterns identified in this study but not explicitly
548 incorporated into performance metrics highlight important future directions for this
549 methodology. For example, changes in spatial patterns of sediment mobility exhibited across
550 flow-form combinations likely influence biological suitability for bed occupation in addition to
551 the magnitude- and timing-based performance metrics considered here. The temporal patterns of
552 bed mobility also varied substantially within the bed occupation and preparation periods (Fig. 7),
553 which was not captured by the selected performance metrics. More information about the spatio-
554 temporal hydraulic requirements for particular species and life-stages and improved metrics for
555 quantifying these characteristics would refine performance estimates within the proposed
556 framework.

557 **4.3 Flow and form controls on ecosystem functioning**

558 Five Mediterranean-montane river ecosystem functions related to geomorphic variability and
559 aquatic habitat were evaluated in the context of interacting flow (i.e., water year type and
560 hydrologic impairment) and form (i.e., morphology type) controls on ecohydraulic response
561 (Figure 5 and 6). Flow convergence routing was controlled primarily by channel form, as it only
562 occurred in the pool-riffle morphology. However, sufficiently high flows were also needed for a
563 shear stress reversal to occur in support of the mechanism. Hydrogeomorphic diversity was
564 controlled primarily by channel form, and specifically topographic variability, as expected. More
565 surprisingly, HMID was also influenced by flow attributes, with water year type, hydrologic
566 impairment, and morphology type all playing significant and interacting roles in the ecohydraulic
567 response. Salmonid bed preparation and occupation illustrate trade-offs in all three controlling
568 variables, with bed preparation performing best in the wet, altered, plane bed scenario while bed
569 occupation performed best in the dry, unimpaired pool-riffle morphology. The duration and
570 timing of redd dewatering risk were controlled by water year type and hydrologic impairment,
571 while the magnitude of dewatering risk, based on the proportion of spawning habitat exhibiting
572 sufficiently low depth or velocity, was controlled solely by channel form. These results
573 emphasize the complex interacting flow and form controls on key ecosystem functions and the
574 differences in dominant controls between ecosystem functions.

575 HMID performance tradeoffs in particular provide insight for environmental water
576 management, given the common conception that increased habitat heterogeneity promotes
577 biodiversity (Dyer and Thoms 2006). The highest HMID was exhibited by the pool-riffle under
578 dry unimpaired conditions. However, under hydrologic impairment, HMID was higher under the

579 wet pool-riffle than the dry plane bed scenario for all but the lowest flows. This finding indicates
580 a tradeoff between flow and form with respect to diversity whereby either increasing topographic
581 variability (i.e., plane bed to pool-riffle) or increasing the number of low flow days in the flow
582 regime (i.e., wet to dry water year type) was capable of increasing overall spatiotemporal
583 diversity. In such instances, knowledge of flow-form interactions could be used to guide more
584 nuanced, targeted management efforts to promote ecological end goals such as increased
585 biodiversity.

586 In general, bed occupation performed poorly across all flow and form scenarios. This finding
587 may be due to the coarse bankfull stage discretization used in the study (eight discharges from
588 0.2 – 2x bankfull stage, Table 1), allowing lower daily discharge values to be associated with
589 higher sediment mobility than occurs in reality. Results such as these can inform future studies
590 by promoting iterative modification of decisions such as the bankfull stage discretization and the
591 range of discharges considered to improve representation of ecosystem functions within the
592 proposed methodology.

593 **4.4 Implications for environmental management**

594 The quantitative metrics of relative performance across a suite of ecosystem functions
595 highlighted critical performance tradeoffs, emphasizing the significance of spatiotemporal
596 diversity of flow and form at multiple scales for maintaining river ecosystem integrity. For
597 example, the pool-riffle morphology supported flow convergence routing and promoted high
598 hydraulic diversity and salmonid bed occupation, while the plane bed morphology supported
599 salmonid bed preparation and provided habitats of reduced dewatering stress for salmonid redds
600 during dry years. These results indicate that restoring or designing a pool-riffle dominated stream
601 network to provide interspersed plane bed reaches may support higher overall ecosystem
602 integrity by promoting distinct and complementary functions in different locations during
603 biologically significant periods. Such findings support the emerging recognition of spatial and
604 temporal heterogeneity as fundamental characteristics of fluvial systems and the need for a
605 flexible framework within which natural processes, such as sediment transport and nutrient
606 dynamics, can occur (Clarke et al. 2003; Gostner, Parasiewicz, et al. 2013; Vanzo et al. 2016;
607 Escobar-Arias and Pasternack 2010).

608 With respect to hydrologic variability, only wet years supported high performance of
609 salmonid bed preparation and shear stress reversals, while dry years significantly increased
610 hydraulic diversity and availability of fall-run Chinook spawning habitat. A range of wet to dry
611 years is required to support the full suite of ecosystem functions considered here. Inter-annual
612 variability plays a key role (in concert with spatial variability of form and bed substrate) in
613 maintaining river ecosystem integrity. This finding also indicates the potential for changes or
614 losses in function under a changing climate in which the spectrum or the ratio of wet to dry years
615 is significantly altered from that to which native riverine species are adapted (Null and Viers
616 2013). For example, fewer sufficiently wet years to generate shear stress reversals in pool-riffle

617 reaches may compromise their ability to maintain high topographic variability, thus shifting the
618 suite of ecosystem functions supported in these reaches towards those already supported by plane
619 bed reaches. This would reduce ecological variability and thus overall ecological resilience of the
620 stream network.

621 This application of synthetic datasets to flow-form-function inquiry provides a foundation for
622 transitioning from expressing ecosystem impacts and responses in terms of fixed flow or form
623 features to spatiotemporally varying hydrogeomorphic dynamics along a spectrum of alterations
624 of the synthetic datasets. The simple, process-based framework proposed here is expected to
625 elucidate key processes and thresholds underlying spatial and temporal dynamics of river
626 ecosystems through future applications. For instance, the functional role and alteration thresholds
627 of individual geomorphic attributes (e.g., confinement, channel bed undulations) could be
628 isolated through iterative generation and evaluation of numerous synthetic channel forms. This
629 information is expected to improve understanding of ecosystem resilience and the potential for
630 rehabilitation projects under current and future hydrogeomorphic alterations.

631 **4.5 Study uncertainty**

632 Uncertainties in the ecosystem functions model developed here include uncertainty in model
633 completeness, parameters, and data inputs. With respect to model completeness, this study
634 explicitly incorporated attributes of key hydrologic and geomorphic processes controlling river
635 ecosystem functions for more complete evaluation of controlling variables and their dynamic
636 interactions. However, several critical aspects of river ecosystems including water quality,
637 temperature, population dynamics, and morphodynamics are not considered in the scope of the
638 current study.

639 Model parameter uncertainties derive from parameter and equation selection. For example,
640 the depth slope product shear stress equation assumes steady uniform flow, which is appropriate
641 for the geomorphic archetypes considered here under steady discharges but should be assessed
642 on a case-by-case basis for application to real channel morphologies (Brown and Pasternack
643 2008; Pasternack et al. 2008). The use of Shields parameter thresholds to delimit sediment
644 transport stages provided a simple approach to explore flow - hydrogeomorphic process
645 relationships, but there is uncertainty associated with these thresholds and others could be
646 selected depending on the application or with more information regarding bed composition. The
647 spatial and temporal thresholds of ERHPs constraining the ecosystem functions are also
648 uncertain. For instance, the requirement of seven consecutive days of flooding for riparian
649 recruitment is an estimate based on field studies across the Sierra Nevada that exhibit high
650 variability between sites.

651 Data input uncertainties originate from the streamflow time series and river corridor
652 morphologies. In the current application, stage-discharge relationships were the main source of
653 hydrologic uncertainty, as they were manually estimated for the Yuba River in the absence of
654 established rating curves. Rating curves derived from field measurements would substantially
655 reduce this source of uncertainty. The use of real streamflow time series minimized uncertainty

656 associate with hydrologic inputs. However, the use of modeled streamflow or hydrologic
657 archetypes, as proposed for future applications, would create additional uncertainty.
658 Uncertainties arising from the use of synthetic river valleys morphologies include field
659 measurements of reach-averaged geomorphic attributes including the CV of width and depth.
660 The frequency and distribution of width and depth measurements used in these calculations will
661 influence variability estimates, and as a result, the synthesized topographies. More research is
662 needed to evaluate the influence of different sampling schemes and measures of topographic
663 variability on the synthesized DTMs and dependent hydrogeomorphic processes.
664

665 **5 Conclusions**

666 This study tackles key questions regarding the utility of synthetic DTMs for ecohydraulic
667 analysis, the ecological significance of topographic variability, how to evaluate the ecological
668 impacts of different flow-form settings or types of river restoration efforts, and whether
669 (re)instatement of key flow or form attributes is likely to restore ecological processes (Council
670 2007). The development and application of simple, quantitative ecosystem performance metrics
671 enabled evaluation of the ecohydraulic response to changes in flow and/or form settings typical
672 of Mediterranean-montane rivers. By comparing these performance metrics across individual and
673 combined adjustments to flow and form attributes, this study provides a novel framework for
674 assessing and comparing ecosystem function performance under natural and human altered flow
675 regimes and river corridor morphologies. Moreover, this research demonstrates the significance
676 of spatiotemporal diversity of *flow* (seasonal and inter-annual) and *form* (channel shape and bed
677 substrate) and their interactions for supporting distinct ecosystem *functions* that maintain river
678 ecosystem integrity.

679

680 **6 Acknowledgements**

681 This research was supported by the UC Davis Hydrologic Sciences Graduate Group
682 Fellowship and the USDA National Institute of Food and Agriculture, Hatch project numbers
683 #CA-D-LAW-7034-H and CA-D-LAW-2243-H. The authors also acknowledge Rocko Brown
684 for instrumental discussions of synthetic river corridors and Helen Dahlke for valuable
685 discussions about hydrology and geomorphology.

686

687

688

689

690 **7 Citations**

- 691
692 Abu-Aly, TR, Gregory B. Pasternack, Joshua R. Wyrick, R Barker, D Massa, and T Johnson. 2014. 'Effects
693 of LiDAR-derived, spatially distributed vegetation roughness on two-dimensional hydraulics in a
694 gravel-cobble river at flows of 0.2 to 20 times bankfull', *Geomorphology*, 206: 468-82.
- 695 Brown, Rocko A., and Gregory B. Pasternack. 2008. 'Engineered channel controls limiting spawning
696 habitat rehabilitation success on regulated gravel-bed rivers', *Geomorphology*, 97: 631-54.
- 697 Brown, Rocko A., and Gregory B. Pasternack. 2014. 'Hydrologic and topographic variability modulate
698 channel change in mountain rivers', *Journal of Hydrology*, 510: 551-64.
- 699 Brown, Rocko A., and Gregory B. Pasternack. 2016. 'Analyzing bed and width oscillations in a self-
700 maintained gravel-cobble bedded river using geomorphic covariance structures', *Earth Surface
701 Dynamics Discussions*: 1-48.
- 702 Brown, Rocko A., and Gregory B. Pasternack. 2017. 'Bed and width oscillations form coherent patterns in
703 a partially confined, regulated gravel-cobble-bedded river adjusting to anthropogenic disturbances',
704 *Earth Surf. Dynam.*, 5: 1-20.
- 705 Brown, Rocko A., Gregory B. Pasternack, and T. Lin. 2015. 'The Topographic Design of River Channels
706 for Form-Process Linkages', *Environmental Management*, 57: 929-42.
- 707 Brown, Rocko A., Gregory B. Pasternack, and W. W. Wallender. 2014. 'Synthetic river valleys: Creating
708 prescribed topography for form-process inquiry and river rehabilitation design', *Geomorphology*, 214:
709 40-55.
- 710 Buffington, John M, and David R Montgomery. 1997. 'A systematic analysis of eight decades of incipient
711 motion studies, with special reference to gravel-bedded rivers', *Water Resources Research*, 33: 1993-
712 2029.
- 713 Caamaño, Diego, Peter Goodwin, John M. Buffington, Jim C. Liou, and Steve Daley-Laursen. 2009.
714 'Unifying criterion for the velocity reversal hypothesis in gravel-bed rivers', *Journal of Hydraulic
715 Engineering*, 135: 66-70.
- 716 Clarke, Stewart J., Lydia Bruce-Burgess, and Geraldene Wharton. 2003. 'Linking form and function:
717 towards an eco-hydromorphic approach to sustainable river restoration', *Aquatic Conservation: Marine
718 and Freshwater Ecosystems*, 13: 439-50.
- 719 Council, National Research. 2007. "River science at the U.S. Geological Survey." In, edited by Committee
720 on River Science at the U.S. Geological Survey, 206. Washington, D.C.
- 721 Cullum, Carola, Gary Brierley, George LW Perry, and Ed TF Witkowski. 2017. 'Landscape archetypes for
722 ecological classification and mapping', *Progress in Physical Geography*, 41: 95-123.
- 723 Doyle, Martin W., Emily H. Stanley, David L. Strayer, Robert B. Jacobson, and John C. Schmidt. 2005.
724 'Effective discharge analysis of ecological processes in streams', *Water Resources Research*, 41.
- 725 Dyer, Fiona J., and Martin C. Thoms. 2006. 'Managing river flows for hydraulic diversity: an example of
726 an upland regulated gravel-bed river', *River Research and Applications*, 22: 257-67.

- 727 Escobar-Arias, M. I., and Gregory B. Pasternack. 2010. 'A hydrogeomorphic dynamics approach to assess
728 in-stream ecological functionality using the functional flows model, part 1-model characteristics', *River
729 Research and Applications*, 26: 1103-28.
- 730 Escobar-Arias, M. I., and Gregory B. Pasternack. 2011. 'Differences in river ecological functions due to
731 rapid channel alteration processes in two California rivers using the functional flows model, part 2-
732 model applications', *River Research and Applications*, 27: 1-22.
- 733 Gasith, A., and B. Resh. 1999. 'Streams in Mediterranean Regions: Abiotic Influences and Biotic Responses
734 to Predictable Seasonal Event', *Annual Review of Ecological Systems*.
- 735 Gostner, Walter, Maria Alp, Anton J. Schleiss, and Christopher T. Robinson. 2013. 'The hydro-
736 morphological index of diversity: a tool for describing habitat heterogeneity in river engineering
737 projects', *Hydrobiologia*, 712: 43-60.
- 738 Gostner, Walter, Peter Parasiewicz, and Anton J. Schleiss. 2013. 'A case study on spatial and temporal
739 hydraulic variability in an alpine gravel-bed stream based on the hydromorphological index of
740 diversity', *Ecohydrology*, 6: 652-67.
- 741 Hanak, Ellen, Jay Lund, Ariel Dinar, Brian Gray, Richard Howitt, Jeffery Mount, Peter Moyle, and Barton
742 Thompson. 2011. "Managing California's Water: From Conflict to Reconciliation." In. San Francisco,
743 CA: Public Policy Institute of California.
- 744 Healey, M.C. 1991. 'Life history of chinook salmon (*Oncorhynchus tshawytscha*).' in C. Groot and L.
745 Margolis (eds.), *Pacific salmon life histories* (University of British Columbia Press: Vancouver, British
746 Columbia).
- 747 Jackson, J. R., G. B. Pasternack, and J. M. Wheaton. 2015. 'Virtual manipulation of topography to test
748 potential pool-riffle maintenance mechanisms', *Geomorphology*, 228: 617-27.
- 749 Jacobson, Robert B., and David L. Galat. 2006. 'Flow and form in rehabilitation of large-river ecosystems:
750 An example from the Lower Missouri River', *Geomorphology*, 77: 249-69.
- 751 Jowett, Ian G. 1993. 'A method for objectively identifying pool, run, and riffle habitats from physical
752 measurements', *New Zealand journal of marine and freshwater research*, 27: 241-48.
- 753 Kasprak, Alan, Nate Hough-Snee, Tim Beechie, Nicolaas Bouwes, Gary Brierley, Reid Camp, Kirstie
754 Fryirs, Hiroo Imaki, Martha Jensen, Gary O'Brien, David Rosgen, and Joseph Wheaton. 2016. 'The
755 Blurred Line between Form and Process: A Comparison of Stream Channel Classification
756 Frameworks', *PLoS One*, 11: e0150293.
- 757 Konrad, Christopher P, Derek B Booth, Stephen J Burges, and David R Montgomery. 2002. 'Partial
758 entrainment of gravel bars during floods', *Water Resources Research*, 38.
- 759 Lai, Young G. 2008. "SRH-2D Version 2: Theory and User's Manual." In. Denver, CO: U.S. Department
760 of the Interior.
- 761 Lane, Belize A., Helen E. Dahlke, Gregory B. Pasternack, and Samuel Sandoval-Solis. 2017. 'Revealing
762 the diversity of natural hydrologic regimes in California with relevance for environmental flows
763 applications', *Journal of American Water Resources Association (JAWRA)*.
- 764 Lane, Belize A., Gregory B. Pasternack, Helen E. Dahlke, and Samuel Sandoval-Solis. 2017. 'The role of
765 topographic variability in river channel classification', *Physical Progress in Geography*.

- 766 MacWilliams, Michael L., Joseph M. Wheaton, Gregory B. Pasternack, Robert L. Street, and Peter K.
767 Kitanidis. 2006. 'Flow convergence routing hypothesis for pool-riffle maintenance in alluvial rivers',
768 Water Resources Research, 42.
- 769 Magilligan, Francis J., and K.H. Nislow. 2005. 'Changes in hydrologic regime by dams', *Geomorphology*,
770 71: 61-78.
- 771 Montgomery, D. R., and J. M. Buffington. 1997. 'Channel reach morphology in mountain basins', *GSA*
772 *Bulletin*.
- 773 Montgomery, D. R., Buffington, J. 1997. 'Channel-reach morphology in mountain rivers'.
- 774 Moyle, Peter B., and Paul J. Randall. 1998. 'Evaluating the Biotic Integrity of Watersheds in the Sierra
775 Nevada, California', *Conservation Biology*, 12: 1318-26.
- 776 Murray, Orla, Martin Thoms, and Scott Rayburg. 2006. "The diversity of inundated areas in semiarid flood
777 plain ecosystems." In *Sediment Dynamics and the Hydromorphology of Fluvial Systems*. Dundee, UK:
778 IAHS Publication.
- 779 Null, Sarah E., and Joshua H. Viers. 2013. 'In bad waters: Water year classification in nonstationary
780 climates', *Water Resources Research*, 49: 1137-48.
- 781 Parasiewicz, Piotr. 2007. 'Using MesoHABSIM to develop reference habitat template and ecological
782 management scenarios', *River Research and Applications*, 23: 924-32.
- 783 Pasternack, Gregory B., Michael K. Bounrisavong, and Kaushal K. Parikh. 2008. 'Backwater control on
784 riffle-pool hydraulics, fish habitat quality, and sediment transport regime in gravel-bed rivers', *Journal*
785 *of Hydrology*, 357: 125-39.
- 786 Pasternack, Gregory Brian. 2011. 2D modeling and ecohydraulic analysis (University of California at
787 Davis).
- 788 Poff, N. LeRoy, and J. V. Ward. 1990. 'Physical habitat template of lotic systems: Recovery in the context
789 of historical pattern of spatiotemporal heterogeneity', *Environmental Management*, 14: 629.
- 790 Poff, N. Leroy; Allan, J. David; Bain, Mark B.; Karr, James R.; Prestegard, Karen L.; Richter, Brian D.;
791 Sparks, Richard E.; Stromberg, Julie C. 1997. 'The natural flow regime: a paradigm for river
792 conservation and restoration', *BioScience*, 47: 769-84.
- 793 Price, Amina E., Paul Humphries, Ben Gawne, Martin C. Thoms, and John Richardson. 2013. 'Effects of
794 discharge regulation on slackwater characteristics at multiple scales in a lowland river', *Canadian*
795 *Journal of Fisheries and Aquatic Sciences*, 70: 253-62.
- 796 Richards, KS. 1976. 'The morphology of riffle-pool sequences', *Earth Surface Processes*, 1: 71-88.
- 797 Richter, Brian D., and Holly E. Richter. 2000. 'Prescribing Flood Regimes to Sustain Riparian Ecosystems
798 along Meandering Rivers
- 799 Prescripción de Regímenes de Inundación para Mantener Ecosistemas Riparios a lo Largo de Ríos
800 Sinuosos', *Conservation Biology*, 14: 1467-78.
- 801 Sandoval-Solis, S, DC McKinney, and DP Loucks. 2010. 'Sustainability index for water resources planning
802 and management', *Journal of Water Resources Planning and Management*, 137: 381-90.

- 803 Scown, MW, MC Thoms, and NR De Jager. 2015. 'An index of floodplain surface complexity', *Hydrology*
804 and *Earth System Sciences Discussions*, 12: 4507-40.
- 805 Small, Melanie J., Martin W. Doyle, Randall L. Fuller, and Rebecca B. Manners. 2008. 'Hydrologic versus
806 geomorphic limitation on CPOM storage in stream ecosystems', *Freshwater Biology*, 53: 1618-31.
- 807 Soulsby, C, AF Youngson, HJ Moir, and IA Malcolm. 2001. 'Fine sediment influence on salmonid
808 spawning habitat in a lowland agricultural stream: a preliminary assessment', *Science of the Total*
809 *Environment*, 265: 295-307.
- 810 Thompson, Alan. 1986. 'Secondary flows and the pool-riffle unit: A case study of the processes of meander
811 development', *Earth Surface Processes and Landforms*, 11: 631-41.
- 812 USFWS. 2010a. "Flow-habitat relationships for spring and fall-run Chinook salmon and steelhead/rainbow
813 trout spawning in the Yuba River." In, 127. Sacramento, CA: The Energy Planning and Instream Flow
814 Branch.
- 815 USFWS. 2010b. "Yuba River Redd Dewatering and Juvenile Stranding Report " In, 60. Sacramento, CA:
816 Energy Planning and Instream Flow Branch, .
- 817 Vanzo, Davide, Guido Zolezzi, and Annunziato Siviglia. 2016. 'Eco-hydraulic modelling of the interactions
818 between hydropeaking and river morphology', *Ecohydrology*, 9: 421-37.
- 819 White, Jason Q., Gregory B. Pasternack, and Hamish J. Moir. 2010. 'Valley width variation influences
820 riffle-pool location and persistence on a rapidly incising gravel-bed river', *Geomorphology*, 121: 206-
821 21.
- 822 Wohl, Ellen, Brian P. Bledsoe, Robert B. Jacobson, N. Leroy Poff, Sarah L. Rathburn, D. M. Walters, and
823 Andrew C. Wilcox. 2015. 'The Natural Sediment Regime in Rivers: Broadening the Foundation for
824 Ecosystem Management', *BioScience*, 65: 358-71.
- 825 Wohl, Ellen, and David Merritt. 2005. 'Prediction of mountain stream morphology', *Water Resources*
826 *Research*, 41.
- 827 Wolman, M. Gordon, and John P. Miller. 1960. 'Magnitude and frequency of forces in geomorphic
828 processes'.
- 829 Worthington, T. A., S. K. Brewer, N. Farless, T. B. Grabowski, and M. S. Gregory. 2014. 'Interacting effects
830 of discharge and channel morphology on transport of semibuoyant fish eggs in large, altered river
831 systems', *PLoS One*, 9: e96599.
- 832 Yarnell, S. M., A. J. Lind, and J. F. Mount. 2012. 'Dynamic flow modelling of riverine amphibian habitat
833 with application to regulated flow management', *River Research and Applications*, 28: 177-91.
- 834 Yoshiyama, Ronald M., Frank W. Fisher, and Peter B. Moyle. 1998. 'Historical Abundance and Decline of
835 Chinook Salmon in the Central Valley Region of California', *North American Journal of Fisheries*
836 *Management*, 18: 487-521.
- 837